

Effect of beam emittance on self-modulation of long beams in plasma wakefield accelerators

K.V.Lotov^{1,2}

¹⁾ Novosibirsk State University, 630090, Novosibirsk, Russia

²⁾ Budker Institute of Nuclear Physics SB RAS, 630090, Novosibirsk, Russia

(Dated: 12 October 2015)

The initial beam emittance determines the maximum wakefield amplitude that can be reached as a result of beam self-modulation in the plasma. The wakefield excited by the fully self-modulated beam decreases linearly with the increase of the beam emittance. There is a value of initial emittance beyond which the self-modulation does not develop even if the instability is initiated by a strong seed perturbation. The emittance scale at which the wakefield is twice suppressed with respect to the zero-emittance case (the so called critical emittance) is determined by inability of the excited wave to confine beam particles radially and is related to beam and plasma parameters by a simple formula. The effect of beam emittance can be observed in several discussed self-modulation experiments.

I. INTRODUCTION

The self-modulation instability^{1,2} (SMI) plays an important role in the concept of proton beam driven plasma wakefield acceleration.^{3,4} This instability transforms a long proton bunch into a train of short micro-bunches spaced one plasma wavelength apart and, therefore, enables efficient excitation of the plasma wave with state-of-the-art proton beams.^{5,6} In turn, proton beams carry enough energy to drive the wave over hundreds of meters and accelerate electrons to energies of 1 TeV and beyond in a single stage.^{3,6-9} This is the main advantage of proton drivers over electron and laser ones for which staging of many plasma sections is necessary to reach this energy scale.¹⁰⁻¹⁴

The SMI works properly only if a selected instability mode is somehow externally seeded.^{2,15-17} Otherwise, non-axisymmetric perturbations (hosing modes) belonging to the same instability family¹⁸ could develop and destroy the beam. Even the axisymmetric modes are sufficient to destroy the beam, if several of them grow concurrently.^{19,20}

Another necessary condition of the long-distance beam propagation is a fine control of the instability with small variations of the plasma density along the beam path. In the perfectly uniform plasma, the seeded instability first transforms the long beam into the train of microbunches, and then heavily destroys them.^{6,21} However, if the beam encounters a small density increase (the plasma density step) at the linear stage of self-modulation, then the stable bunch train is formed which propagates in the plasma up to the beam energy depletion.⁶ Also, a gentle growth of the plasma density is favorable for trapping the witness electrons into optimal phases of the wave.²² Irregular or small scale density perturbations are, however, undesirable, as they are fatal for electrons accelerated by the excited wakefield.^{23,24}

By now, the properties of the SMI are known mostly from numerical simulations. The mechanism of bunch destruction in uniform plasmas and the role of the plasma density step are well understood, but for high

quality beams only.²⁵ Available analytical models are limited to narrow beams and the linear stage of the instability,^{2,26-28} with the primary attention given to the interplay of SMI and hosing modes.²⁹⁻³¹ Experimental evidences of the SMI that come from electron or positron beams are too fragmentary for detailed comparison with the theory.^{32,33} The ultimate test of SMI properties will be possible with the AWAKE experiment^{4,34-36} that is now under preparation at CERN. Several smaller scale experiments with electron beams³⁷⁻⁴² are also discussed or prepared and may give valuable information.

In this paper, we numerically study the dependence of SMI properties on beam parameters, the most important of which is the beam emittance. Earlier studies of this kind⁴³ were limited to the parameter area of interest for the AWAKE experiment at which the instability is mixed with many other effects. Here we study the SMI in the purest form and formulate universal limitations for it. In Sec.II, we define the problem under study and describe the test case that we take as an example. We then consider the uniform plasma in Sec.III and the plasma with the density step in Sec.IV. In Sec.V, we discuss which of the proposals for experimental SMI studies may suffer from too large beam emittances.

II. STATEMENT OF THE PROBLEM

We consider the same idealized setup as in Ref. [25] and use the same units of measure: speed of light c for velocities, electron mass m for masses, elementary charge e for charges, initial plasma density n_0 for densities, inverse plasma frequency ω_p^{-1} for times, plasma skin depth c/ω_p for distances, and wavebreaking field $E_0 = mc\omega_p/e$ for fields. We also use cylindrical coordinates (r, φ, z) and the co-moving coordinate $\xi = z - ct$.

Our aim is to induce general scalings from particular cases. For this, we simulate mono-energetic positron

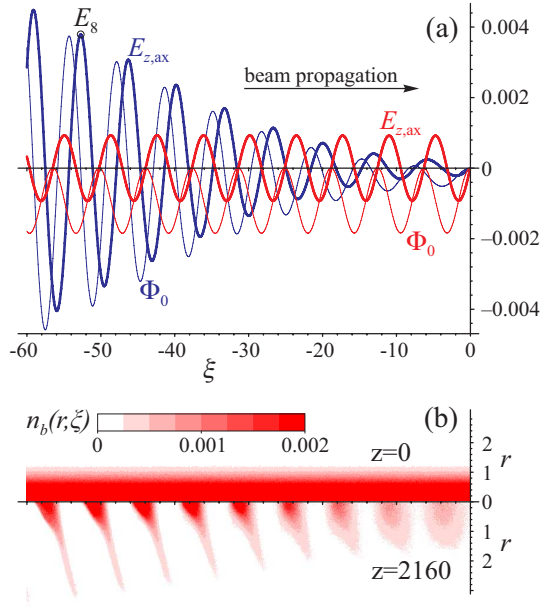


FIG. 1. (a) The on-axis electric field $E_{z,ax}$ (thick lines) and the depth of the radial potential well Φ_0 (thin lines) at the beginning of interaction at $z = 0$ (red) and at the moment of the strongest wakefield at $z = 2160$ (blue) for the default beam parameters; (b) the beam density $n_b(r, \xi)$ at these propagation distances.

beams with the initial density profile

$$n_b = \begin{cases} n_{b0} e^{-r^2/(2\sigma_r^2)}, & -L < \xi < 0, \\ 0, & \text{otherwise,} \end{cases} \quad (1)$$

which propagate in the positive z direction through the cold, radially uniform plasma with immobile ions. Thus we exclude effects of ion motion^{44,45} and radial plasma non-uniformity^{46,47} from our consideration. We vary the relativistic factor γ_b , radius σ_r , density n_{b0} , length L , and emittance ε_b of the beam in the neighborhood of some default values $\gamma_b = 1000$, $\sigma_r = 0.5$, $n_{b0} = 0.004$, $L = 60$, and $\varepsilon_b = \varepsilon_{b0} = 4.65 \times 10^{-4}$. We intentionally consider only small beam densities to keep the plasma response linear and exclude effects of plasma non-linearity^{43,48} that may complicate the process.

We simulate the test cases with the axisymmetric quasi-static 2d3v hybrid code LCODE^{49,50}, in which the beam is modeled with macro-particles, and plasma is treated as the electron fluid.

The process of beam self-modulation looks as follows. The hard leading edge leaves behind a seed wakefield [Fig. 1(a)] that periodically focus or defocus beam slices. Perturbations of the beam radius and the plasma wave amplify each other and grow in space (in negative ξ direction) and in time [Figs. 1(a) and 2]. Concurrently, the emittance driven divergence reduces the beam density at cross-sections of weak focusing [Fig. 1(b)]. At the time of full beam bunching, the excited wakefield reaches its maximum value and then decreases due to partial de-

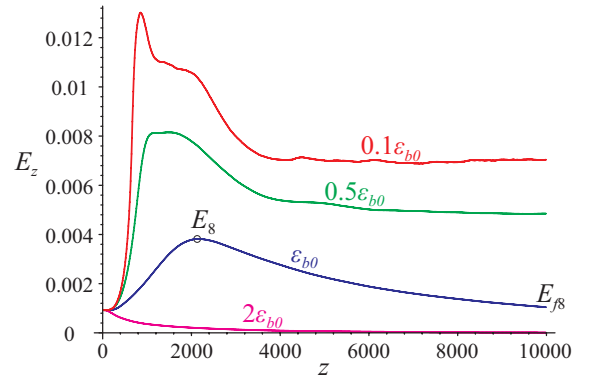


FIG. 2. The electric field at the 8th local maximum (inside the 8th micro-bunch) as a function of propagation distance for beams of various emittance.

struction of the micro-bunches. The typical behavior of the wave amplitude at the 8th local maximum (inside the 8th micro-bunch) is shown in Fig. 2 for several values of the initial beam emittance. Since the figure of merit for the self-modulation is the longitudinal field excited by the bunched beam, we focus our attention on the on-axis field E_j at certain (numbered by the subscript j) local field maxima in ξ and absolute maximum in z . This field maximum is located inside the j -th micro-bunch. The corresponding points for the default beam parameters are shown in Figs. 1(a) and 2 by small circles. As we see from Fig. 2, the wave amplitude does not always flatten out at large z . The amplitude E_{fj} at long propagation distances $z = 10000$ (which was analyzed in Ref. [25]) thus loses its significance for highly divergent beams, although it still contains some important information about the process.

III. UNIFORM PLASMA

As we see from Fig. 2, the maximum wakefield excited by the self-modulating beam strongly depends on the initial beam emittance. This dependence is close to the linear one (Fig. 3) and can be conveniently characterized by

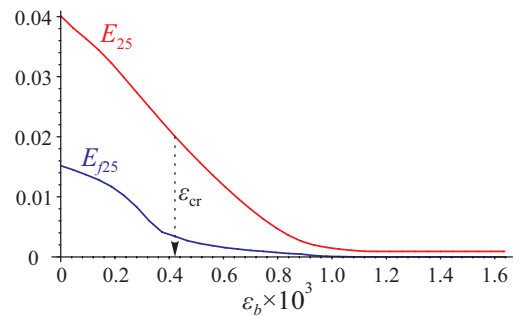


FIG. 3. The electric field at the distance of the strongest self-modulation (E_{25}) and at the long distance point (E_{f25}) as functions of the beam emittance for the default beam parameters.

the critical emittance ε_{cr} that we define as the emittance at which the maximum field is reduced twice compared to the zero-emittance beam. The wave amplitude at long distances E_{fi} drops down at the same emittance scale. The default emittance ε_{b0} was deliberately chosen such that $\varepsilon_{b0} \approx \varepsilon_{\text{cr}}$ for $j = 25$.

The ratio of the beam emittance to the critical emittance is thus an important beam feature that shows whether or not the particular beam can self-modulate efficiently. Let us relate the critical emittance to other (usually tabulated) beam parameters.

Two effects could be responsible for low fields at high emittances:⁶ beam dilution due to its divergence during development of the SMI and inability of the excited wave to confine beam particles radially. To analyze the first one, we estimate the time at which a beam particle shifts transversely by the distance of about σ_r ; it is

$$t_{\text{diverg}} \sim \sigma_r^2 / \varepsilon_b. \quad (2)$$

The characteristic time of SMI growth is²⁶

$$t_{\text{growth}} \propto \sqrt{\frac{\gamma_b}{Ln_{b0}}}. \quad (3)$$

This expression differ from the commonly used ones²⁶ in that we explicitly include the dependence on the beam length L into the growth time. Equating the two times yields the scaling

$$\varepsilon_{\text{cr}} \propto \sigma_r^2 \sqrt{\frac{Ln_{b0}}{\gamma_b}}. \quad (4)$$

For the second effect, we compare the energy of transverse motion of a beam particle⁶

$$W_{\text{tr}} = \frac{\varepsilon_b^2 \gamma_b}{2\sigma_r^2} \quad (5)$$

and the depth of the potential well Φ_0 that we calculate more precisely than in Ref. [6]. If the beam density is factorable and has the form

$$n_b(r, \xi) = n_{b0} f(r) g(\xi), \quad (6)$$

then the force \vec{F} acting on an axially moving relativistic positron is also factorable,

$$\vec{F} \equiv \vec{E} + [\vec{e}_z, \vec{B}] = -\nabla \Phi(r, \xi) = -\nabla (n_{b0} F(r) G(\xi)), \quad (7)$$

where \vec{e}_z is the unit vector in z -direction, and expressions for $F(r)$ and $G(\xi)$ can be found, e.g., in Refs. [51–53]. The density of the self-modulating beam is not factorable [Fig. 1(b)], so the best estimate we can make for Φ_0 is to assume that $G(\xi)$ oscillates with a linearly growing amplitude [as in Fig. 1(a)], and $F(0)$ is the same as for the initial Gaussian beam:⁵³

$$F(0) = \frac{\sigma_r^2}{2} e^{\sigma_r^2/2} \Gamma(0, \sigma_r^2/2), \quad (8)$$

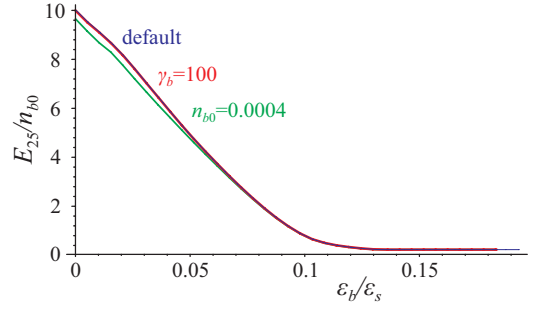


FIG. 4. The normalized dependence of the maximum accelerating field inside the 25-th micro-bunch (E_{25}) on the beam emittance for the default parameter set (blue) and for beams of 10 times lower energy (red) or density (green).

where

$$\Gamma(\alpha, \beta) = \int_{\beta}^{\infty} t^{\alpha-1} e^{-t} dt. \quad (9)$$

Collecting these expression together, we find

$$\Phi_0 \propto \Phi_{\text{sc}} \equiv n_{b0} L \sigma_r^2 e^{\sigma_r^2/2} \Gamma(0, \sigma_r^2/2), \quad (10)$$

and, by equating the amplitude of Φ_0 and W_{tr} ,

$$\varepsilon_{\text{cr}} \propto \sigma_r^2 \sqrt{\frac{Ln_{b0}}{\gamma_b}} e^{\sigma_r^2/2} \Gamma(0, \sigma_r^2/2). \quad (11)$$

If we consider the j -th field maximum, we take the coordinate $|\xi|$ of this maximum as L .

To check the correctness of the obtained scalings, we denote the right-hand side of (11) by ε_s and compare it with simulation results. The scalings with beam energy γ_b and density n_{b0} are remarkably precise (Fig. 4), and even the shape of the curve remains unchanged by order of magnitude variations of γ_b and n_{b0} . The scalings with the beam radius σ_r and length L are correct everywhere except for short narrow beams (Fig. 5). This figure also shows the numerical factor missed in derivation of (11): $\varepsilon_{\text{cr}} \approx 0.05 \varepsilon_s$.

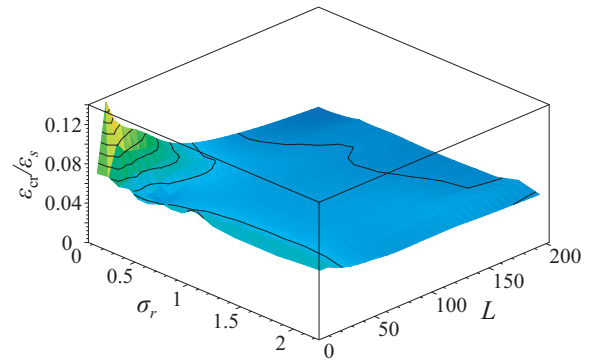


FIG. 5. Correctness of the scaling (11) for beams of various radius σ_r and length L .

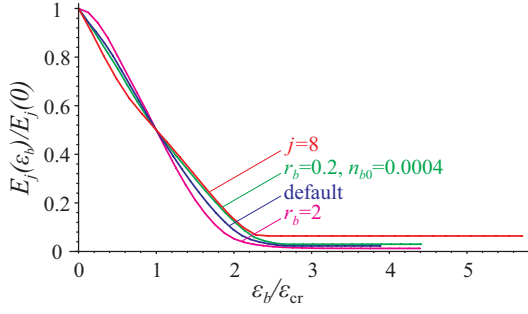


FIG. 6. The normalized dependence of the maximum accelerating field on the beam emittance for various beams. Beam parameters that differ from the default case (25-th local maximum) are indicated.

The scaling (4) is, obviously, incorrect. Consequently, the reduction of the maximum wakefield at high beam emittances happens because the wakefield of the self-modulated beam is not strong enough to confine all beam particles tightly focused. The wakefield reduction with respect to the idealized zero-emittance beam thus depends on the single parameter only, the ratio of the beam emittance to the critical emittance, in a wide interval of other beam parameters (Fig. 6). If the beam particles are not positrons and have the mass m_b , then the critical emittance for this beam is

$$\varepsilon_{\text{cr}} \approx 0.05 \sigma_r^2 \sqrt{\frac{L n_{b0}}{m_b \gamma_b}} e^{\sigma_r^2/2} \Gamma(0, \sigma_r^2/2). \quad (12)$$

The formula (12) may be misleading in that it implicitly contains the plasma density through units of measure. In terms of the beam current $I_b = n_{b0} \sigma_r^2/2$, beam energy $W_b = m_b \gamma_b$, beam length measured in wave periods $j \approx L/(2\pi)$, and in conventional units it is more informative:

$$\varepsilon_{\text{cr}} \approx 0.18 \sigma_r \sqrt{j \frac{e I_b}{m c^3} \frac{m c^2}{W_b} e^{\omega_p^2 \sigma_r^2/(2c^2)} \Gamma\left(0, \frac{\omega_p^2 \sigma_r^2}{2c^2}\right)}. \quad (13)$$

Of importance is thus the initial angular spread of the beam $\delta\alpha = \varepsilon_b/\sigma_r$, the critical value for which is

$$\alpha_{\text{cr}} \approx \sqrt{j \frac{e I_b}{m c^3} \frac{m c^2}{W_b}} F\left(\frac{\omega_p^2 \sigma_r^2}{2c^2}\right) \quad (14)$$

with the dimensionless function $F(x)$ shown in Fig. 7. For the most interesting case of $\sigma_r \approx c/\omega_p$, $F(x) \approx 0.2$.

IV. PLASMA WITH A DENSITY STEP

A small step-like increase δn of the plasma density at the linear stage of SMI development results in formation of the bunch train that stably propagates in the plasma for a long distance^{6,25}. The established wave amplitude

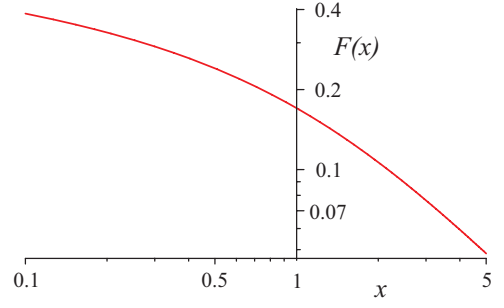


FIG. 7. The dimensionless function $F(x)$ for the critical beam divergence (14).

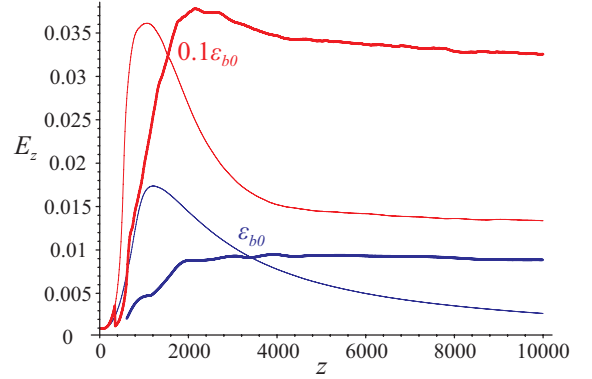


FIG. 8. The electric field at the 25th local maximum (inside the 25th micro-bunch) as a function of propagation distance for beams of various emittance with (thick lines) and without (thin lines) the plasma density step. The step parameters are optimized for the maximum field at $z = 10000$.

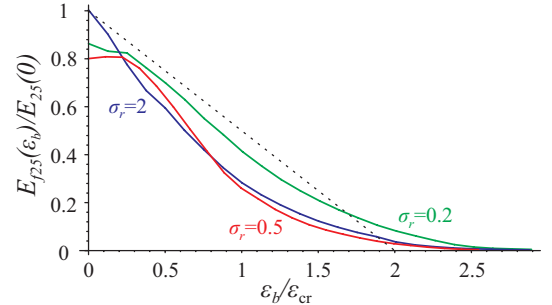


FIG. 9. The normalized dependence of the established accelerating field E_{j25} on the beam emittance for the plasma with the optimized density step and beams of various radius (indicated on the plot). The field is normalized to the maximum field in the uniform plasma at zero emittance. The dash line shows the linear decrease typical for $E_j(\varepsilon_b)$.

in this case also depends on the initial beam emittance (Fig. 8). The emittance scale for the twofold reduction of the established wakefield is the same, ε_{cr} , though the law of field reduction may differ from the linear one (Fig. 9). A large beam emittance also changes the optimum location z_s of the step [Fig. 10(a)]. The optimum location corresponds to the linear stage of the instability²⁵, so the

TABLE I. Proposals for SMI experiments

Facility, reference	L , cm	σ_r , μm	I_b , A	W_b , GeV	ε_b , mm mrad	n_0 , cm^{-3}	j	$\varepsilon_b/\varepsilon_{\text{cr}}$	A_{nl}
PITZ (DESY, Zeuthen) ³⁷	0.593	42	5	0.0215	0.009	10^{15}	5	0.07	0.05
FACET (SLAC, Stanford) ³⁹	0.1	10	770	20.5	0.0012	2.3×10^{17}	14	0.12	1.6
LHC (CERN, Geneva) ⁶	8	100	27	7000	0.0005	3×10^{15}	130	0.17	0.4
AWAKE (CERN, Geneva) ³⁶	12	200	50	400	0.009	7×10^{14}	95	0.3	0.5
IC VEPP-5 (BINP, Novosibirsk) ³⁸	1.6	20	60	0.511	0.023	5×10^{14}	11	0.3	11
PS (CERN, Geneva) ⁵	40	400	10	24	0.08	5×10^{14}	270	0.8	0.1
ATF (BNL, Brookhaven) ⁴¹	0.096	120	310	0.0583	0.11	3.03×10^{16}	5	1.05	0.01
PROTOPLASMA (Fermilab, Batavia) ⁵⁴	20	100	20	120	0.03	10^{16}	600	1.4	0.4

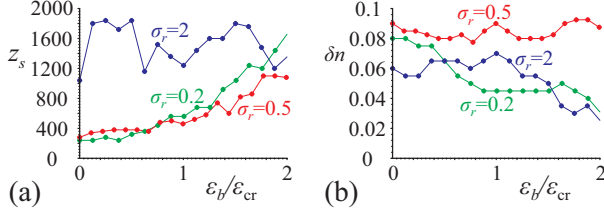


FIG. 10. Optimum location (a) and magnitude (b) of the density step as functions of the beam emittance for beams of different radius (indicated on the plots). The step parameters are optimized for the maximum E_{f25} . Points are obtained from simulations, connecting lines are added for visibility.

slower wave growth observed at large radii or emittances of the beam results in later optimum steps. The optimum magnitude δn does not show any significant trend [Fig. 10(b)], as it is determined by the beam length L , which does not change.

V. AVAILABLE DRIVE BEAMS

Let us apply the obtained formulae to beams that have been discussed in the context of self-modulation studies. The key parameters of proposed experiments are listed in Table I. The parameter L is the beam length for flattop beams, $L = 2\sigma_z$ for Gaussian beams (σ_z is the root-mean-square beam length), and $L = \sigma_z$ for proposals with half-cut beams (AWAKE, LHC). We see that several cases have $\varepsilon_b/\varepsilon_{\text{cr}} \gtrsim 1$, so the emittance driven erosion may suppress self-modulation there.

The last column of Table I shows whether the above linear theory is applicable to these beams or not. As a quick measure of nonlinearity we take

$$A_{\text{nl}} = j n_{b0}. \quad (15)$$

This is the estimated perturbation of the plasma density by j micro-bunches of the density n_{b0} that resonantly drive the wave. The linear approximation violates at $A_{\text{nl}} \sim 0.5$ by the nonlinear elongation of the plasma wave⁴⁸. If $A_{\text{nl}} \gg 1$, then the beam-plasma interaction

is strongly nonlinear, and hosing modes may dominate self-modulation even if the latter is properly seeded³¹.

ACKNOWLEDGMENTS

This work is supported by The Russian Science Foundation, grant No. 14-12-00043. The computer simulations are made at Siberian Supercomputer Center SB RAS.

- ¹K.V.Lotov, Instability of long driving beams in plasma wakefield accelerators. Proc. 6th European Particle Accelerator Conference (Stockholm, 1998), p.806-808.
- ²N.Kumar, A.Pukhov, and K.Lotov, Phys. Rev. Lett. **104**, 255003 (2010).
- ³A.Caldwell, K.Lotov, A.Pukhov, and F.Simon, Nature Phys. **5**, 363 (2009).
- ⁴R.Assmann, R.Bingham, T.Bohl, C.Bracco, B.Buttenschon, A.Butterworth, A.Caldwell, S.Chattopadhyay, S.Cipiccia, E.Feldbaumer, et al. (AWAKE Collaboration), Plasma Phys. Control. Fusion **56**, 084013 (2014).
- ⁵A. Caldwell, K. Lotov, A. Pukhov and G. Xia, Plasma Phys. Controlled Fusion **53**, 014003 (2011).
- ⁶A. Caldwell and K. V. Lotov, Phys. Plasmas **18**, 103101 (2011).
- ⁷K.V.Lotov, Phys. Rev. ST Accel. Beams **13**, 041301 (2010).
- ⁸L.Yi, B.Shen, K.Lotov, L.Ji, X.Zhang, W.Wang, X.Zhao, Y.Yu, J.Xu, X.Wang, Y.Shi, L.Zhang, T.Xu, Z.Xu, Phys. Rev. ST Accel. Beams **16**, 071301 (2013).
- ⁹L.Yi, B.Shen, , L.Ji, K.Lotov, A.Sosedkin, X.Zhang, W.Wang, J.Xu, Y.Shi, L.Zhang, and Z.Xu, Scientific Reports **4**, 4171 (2014).
- ¹⁰A.M.Kudryavtsev, K.V.Lotov, A.N.Skrinsky, Nuclear Instr. Meth. A **410**, 388 (1998).
- ¹¹J.Rosenzweig, N.Barov, A.Murokh, E.Colby, P. Colestock, Nuclear Instr. Meth. A **410**, 532 (1998).
- ¹²C. B. Schroeder, E. Esarey, C. G. R. Geddes, C. Benedetti, and W. P. Leemans, Phys. Rev. ST Accel. Beams **13**, 101301 (2010).
- ¹³K.Nakajima, A.Deng, X.Zhang, B.Shen, J.Liu, R.Li, Z.Xu, T.Ostermayr, S.Petrovics, C.Klier, K.Iqbal, H.Ruhl, and T.Tajima, Phys. Rev. ST Accel. Beams **14**, 091301 (2011).
- ¹⁴C.B.Schroeder, E.Esarey, and W.P.Leemans, Phys. Rev. ST Accel. Beams **15**, 051301 (2012).
- ¹⁵G. Xia, A. Caldwell, K. Lotov, A. Pukhov, N. Kumar, W. An, W. Lu, W. B. Mori, C. Joshi, C. Huang, P. Muggli, R. Assmann, F. Zimmermann, AIP Conf. Proc. **1299**, 510 (2010).
- ¹⁶K.V.Lotov, G.Z.Lotova, V.I.Lotov, A.Upadhyay, T.Tuckmantel, A.Pukhov, A.Caldwell, Phys. Rev. ST Accel. Beams **16**, 041301 (2013).

- ¹⁷C.Siemon, V.Khudik, S.A.Yi, A.Pukhov, and G.Shvets, Phys. Plasmas **20**, 103111 (2013).
- ¹⁸J.Krall and G.Joyce, Phys. Plasmas **2**, 1326 (1995).
- ¹⁹K.V.Lotov, Nuclear Instr. Methods A **410**, 461 (1998).
- ²⁰J.Vieira, L.D.Amorim, Y.Fang, W.B.Mori, P.Muggli, and L.O.Silva, Plasma Phys. Control. Fusion **56**, 084014 (2014).
- ²¹K.V.Lotov, Phys. Plasmas **18**, 024501 (2011).
- ²²A.Petrenko, private communications (2015).
- ²³C.B.Schroeder, C.Benedetti, E.Esarey, F.J.Gruener, and W. P. Leemans, Phys. Plasmas **19**, 010703 (2012).
- ²⁴K.V.Lotov, A.Pukhov, and A.Caldwell, Phys. Plasmas **20**, 013102 (2013).
- ²⁵K. V. Lotov, arXiv:1503.05104 [physics.plasm-ph] (to appear in Phys. Plasmas).
- ²⁶A. Pukhov, N. Kumar, T. Tuckmantel, A. Upadhyay, K. Lotov, P. Muggli, V. Khudik, C. Siemon, and G. Shvets, Phys. Rev. Lett. **107**, 145003 (2011).
- ²⁷C.B.Schroeder, C.Benedetti, E.Esarey, F.J.Gruener, and W. P. Leemans, Phys. Rev. Lett. **107**, 145002 (2011).
- ²⁸A.Pukhov, T.Tuckmantel, N.Kumar, A.Upadhyay, K.Lotov, V.Khudik, C.Siemon, G.Shvets, P.Muggli, and A.Caldwell, AIP Conf. Proc. **1507**, 103 (2012).
- ²⁹C.B.Schroeder, C.Benedetti, E.Esarey, F.J.Gruener, and W.P.Leemans, Phys. Rev. E **86**, 026402 (2012).
- ³⁰C.B.Schroeder, C.Benedetti, E.Esarey, F.J.Gruener, and W.P.Leemans, Phys. Plasmas **20**, 056704 (2013).
- ³¹J. Vieira, W. B. Mori, and P. Muggli, Phys. Rev. Lett. **112**, 205001 (2014).
- ³²M.J.Hogan, C.E.Clayton, C.Huang, P.Muggli, S.Wang, B.E.Blue, D.Walz, K.A.Marsh, C.L.O'Connell, S.Lee, R.Iverson, F.J.Decker, P.Raimondi, W.B.Mori, T.C.Katsouleas, C.Joshi, and R.H.Siemann, Phys. Rev. Lett. **90**, 205002 (2003).
- ³³Y. Fang, V. E. Yakimenko, M. Babzien, M. Fedurin, K. P. Kusche, R. Malone, J. Vieira, W. B. Mori, and P. Muggli, Phys. Rev. Lett. **112**, 045001 (2014).
- ³⁴R. Tarkeshian, Proton electron accelerator at CERN. Proceedings of IPAC2014 (Dresden, Germany), p.1537-1539.
- ³⁵C.Bracco, E.Gschwendtner, A.Petrenko, H.Timko, T.Argyropoulos, H.Bartosik, T.Bohl, J.E.Mueller, B.Goddard, M.Meddahi, A.Pardons, E.Shaposhnikova, F.M.Velotti, H.Vincke, Nucl. Instr. Meth. A **740**, 48 (2014).
- ³⁶K.V.Lotov, A.P.Sosedkin, A.V.Petrenko, L.D.Amorim, J.Vieira, R.A.Fonseca, L.O.Silva, E.Gschwendtner, and P.Muggli, Phys. Plasmas **21**, 123116 (2014).
- ³⁷M.Gross, R.Brinkmann, J.D.Good, F.Grüner, M.Khojayan, A.Martinez de la Ossa, J.Osterhoff, G.Pathak, C.Schroeder, F.Stephan, Nucl. Instr. Meth. A **740**, 74 (2014).
- ³⁸A. V. Petrenko, K. V. Lotov, P. V. Logatchov and A. V. Burdakov, AIP Conf. Proc. **1299**, 467 (2010).
- ³⁹J. Vieira, Y. Fang, W. B. Mori, L. O. Silva, and P. Muggli, Phys. Plasmas **19**, 063105 (2012).
- ⁴⁰P. Muggli, O. Reimann, L.D. Amorim, N.C. Lopes, J.M. Vieira, S.J. Gessner, M. Hogan, S.Z. Li, M.D. Litos, K. Marsh, W. Mori, C. Joshi, N. Vafaei-Najafabadi, E. Adli, V.K. Berglyd Olsen, Electron bunch self-modulation in a long plasma at SLAC FACET. Proceedings of IPAC2014 (Dresden, Germany), p.1476-1478.
- ⁴¹Y.Fang, W.Mori, and P.Muggli, AIP Conf. Proc. **1507**, 559 (2012).
- ⁴²P.Muggli, B.Allen, Y.Fang, V.Yakimenko, M.Babzien, K.Kusche, M.Fedurin, J.Vieira, J.Martins, and L.Silva, AIP Conf. Proc. **1507**, 594 (2012).
- ⁴³K.V.Lotov, V.A.Minakov, and A.P.Sosedkin, Phys. Plasmas **21**, 083107 (2014).
- ⁴⁴J.Vieira, R.A.Fonseca, W.B.Mori, and L.O.Silva, Phys. Rev. Lett. **109**, 145005 (2012).
- ⁴⁵J. Vieira, R. A. Fonseca, W. B. Mori, and L. O. Silva, Phys. Plasmas **21**, 056705 (2014).
- ⁴⁶Y. Fang, J. Vieira, L. D. Amorim, W. Mori, and P. Muggli, Phys. Plasmas **21**, 056703 (2014).
- ⁴⁷K.V.Lotov, A.P.Sosedkin, A.V.Petrenko, Phys. Rev. Lett. **112**, 194801 (2014).
- ⁴⁸K.V.Lotov, Phys. Plasmas **20**, 083119 (2013).
- ⁴⁹K.V.Lotov, Phys. Plasmas **5**, 785 (1998).
- ⁵⁰See www.inp.nsk.su/~lotov/lcode for code description and manual.
- ⁵¹R.Keinigs and M.E.Jones Phys. Fluids **30**, 252 (1987).
- ⁵²E.Esarey, P.Sprangle, J.Krall, and A.Ting, IEEE Trans. Plasma Sci. **24**, 252 (1996).
- ⁵³W. Lu, C. Huang, M. M. Zhou, W. B. Mori, and T. Katsouleas, Phys. Plasmas **12**, 063101 (2005).
- ⁵⁴J.C.T.Thangaraj, C.S.Park, J.D.Lewis, P.Spentzouris, W.An, W.Mori, and C.Joshi, AIP Conf. Proc. **1507**, 644 (2012).